ISSN 0915-633X

9.12.9

900 y

NATIONAL INSTITUTE FOR FUSION SCIENCE

A Forced Gas-Cooled Single-Disk Window Using Silicon Nitride Composite for High Power CW Millimeter Waves

T. Shimozuma, S. Morimoto, M. Sato, Y. Takita, S. Ito, S. Kubo, H. Idei, K. Ohkubo and T. Watari

(Received - Oct. 3, 1997)

NIFS-514 Oct. 1997

RESEARCH REPORT
NIFS Series

NAGOYA, JAPAN

A FORCED GAS-COOLED SINGLE-DISK WINDOW USING SILICON NITRIDE COMPOSITE FOR HIGH POWER CW MILLIMETER WAVES

T. Shimozuma, S. Morimoto[1)], M. Sato, Y. Takita, S. Ito,
S. Kubo, H. Idei, K. Ohkubo and T. Watari

National Institute for Fusion Science
322-6, Oroshi-cho, Toki-shi, Gifu, 509-52, Japan
1) Kanazawa Institute of Technology
7-1, Oogigaoka, Nonoichi, Ishikawa, 921, Japan

Abstract

Silicon nitride composite as a candidate of a window material for high power CW (Continuous Wave) millimeter-waves was high power tested especially with a surface cooling by impinging gas nitrogen jets on the single-disk surface. Gas-cooling dramatically suppressed the temperature of the window disk even with gas flow rate of around 100 l/min. With gas cooling of 465l/min., 130kW CW power of HE_{11} mode could be transmitted through the silicon nitride window with a diameter of 88.9mm. The peak window temperature was completely saturated on 123.6 °C. Without gas-cooling it did not saturate and reached 323 °C during 30 seconds pulse. A possibility of 1MW CW single disk Brewster windows with a forced gas-cooling is discussed, resulting in convinced prospects of the windows with realistic size and thickness.

Keywords

gyrotron, vacuum barrier window, silicon nitride, gas-cooling,
electron cyclotron heating

Submitted to International Journal of Infrared and Millimeter Waves

1. Introduction

A vacuum barrier window is one of the most critical component to realize high power CW (Continuous Wave) gyrotrons[1]. Many efforts to accomplish 1 MW CW windows have been made all over the world. The key of the high power window design is how to keep the thermal and mechanical stresses in the dielectric disk small by reducing and removing the deposited heat as effectively as possible.

The concept of the windows could be divided into two groups, such as multiple-disk windows with a surface (or substantial) cooling and single-disk ones with a circumference cooling. The surface-cooling can reduce the thermal stresses in the window. With an FC-75(3M), which is a low microwave absorbing liquid, it was demonstrated that a surface-cooled double-disk sapphire window had a performance of CW operation up to 400 kW. At the power level of 400kW, the disk temperature rise reached around the boiling limit of the cooling liquid[2,3]. A distributed window is another concept of the substantial cooling. A 1 MW equivalent power could be transmitted through the window[4,5]. However, the fabrication of the larger size one with real 1 MW capability has not been succeeded.

Single-disk windows have a merit of simple structures which assure higher reliability than complicated multiple-disk designs. The peak temperature of the single-disk windows which are made of conventional materials such as alumina, sapphire and boron nitride continues to rise during the operation; for example, the temperature of a boron nitride 140 GHz window rose up to 700 °C. in 2 sec. pulse at 650kW output level[6]. For CW operation, cryogenically cooled single-disk windows were tested using sapphire or Au-doped silicon. When these materials are cooled down to the cryogenic temperature, the loss tangent decreases in one or two order lower and the thermal conductivity increases in one order higher than at room temperature[7-9]. The CVD diamonds (diamond like carbon) are believed as the idealistic material because of its very high thermal conductivity[10]. The loss tangent and mechanical reliability depend on the purity of the diamond.

If we would combine the concept of the effective surface-cooling and the simple structure of a single-disk window, we could realize CW windows. By means of the gas-cooling, the surface-cooled single-disk window might be possible to persist in CW power transmission.

A new sintered silicon nitride composite (SN-287) has been developed by Kyocera corporation in Japan. It has higher thermal shock resistance, higher flexural strength and better thermal conductivity than sapphire. The loss tangent is comparable to sapphire[11]. Table 1 presents the physical, electrical and mechanical characteristics of the silicon nitride in comparison with C-cut sapphire.

We fabricated a single-disk window, which had an 88.9 mm effective diameter, with a surface-cooling mechanism by obliquely impinging gas jets on the disk. It was tested in the 150 kW, HE_{11}, 84 GHz transmission line where the power flux density exceeded 8 kW/cm^2 on the center of the

Table 1 Comparison of physical, electrical and mechanical characteristics between a silicon nitride composite and a C-cut sapphire

	uint	Silicon Nitride Composite	Sapphire (⊥C)
Density	g/cm^3	3.4	4.0
Modulus of Elasticity	GPa	318	470
Poisson Ratio		0.28	0.3
Linear Expansion Coeff.	$\times 10^{-6}$/K	2.4	4.5
Thermal Conductivity	W/mK	59	42
Specific Heat Capacity	J/gK	0.63	0.75
Dielectric Constant		7.9	9.4
Loss Tangent	$\times 10^{-4}$	1.0 (30-40GHz, R.T.) 1-1.5 (84GHz, R.T.) 2.4 (140-145GHz, R.T.)	1.9 (140GHz, R.T.)
Dielectric Strength	$\times 10^4$ kV/m	1.85	4.8
Bending Strength	MPa	800	500
Compressive Strength	MPa	5000 - 6000	2950
Thermal Shock Resistance		>750 deg.C (Melting solder)	
Metalizing/Brazing		OK	OK
Possible size		ϕ400mm	ϕ270mm, 250x75mm
Cost		less expensive	expensive

window. The window peak temperature saturated in about 15 sec. at around 120 °C. with gas-cooling, while it continuously increased up to 320 °C at the end of 30 sec. pulse without gas-cooling. The gas-jet-cooling demonstrated to handle the power flux density of 8 kW/cm^2 substantially in steady state. It is expected that an elongated window such as a Brewster window with the gas-jet-cooling can handle 1MW CW power in the waveguide with an effective diameter of 140mm even for a peaky profile as the HE_{11} mode.

This paper is organized as follows. The structure of the test window are described in Sec. 2. In Sec. 3 the experimental setup for high power window testings is explained in detail. Experimental results are given in Sec. 4. In Sec. 5 a temperature gradient, estimation of heat transfer coefficient, and a Brewster window for 1MW CW window are discussed. Finally, Section 6 is devoted to the summary of the paper.

2. Forced gas-cooled single-disk window

From a viewpoint of safety and damage in windows attached to the plasma experimental device such as Large Helical Device (LHD), double-disk windows surface-cooled by FC-75 are not preferable to single-disk windows. The single-disk windows, however, cannot be used for CW operation at high power level, because of the inferiority of its thermal conductivity. Larger diameter, more flattened RF profile and/or another surface-cooling for the window are required for a several hundred kilowatts to one megawatt CW power transmission.

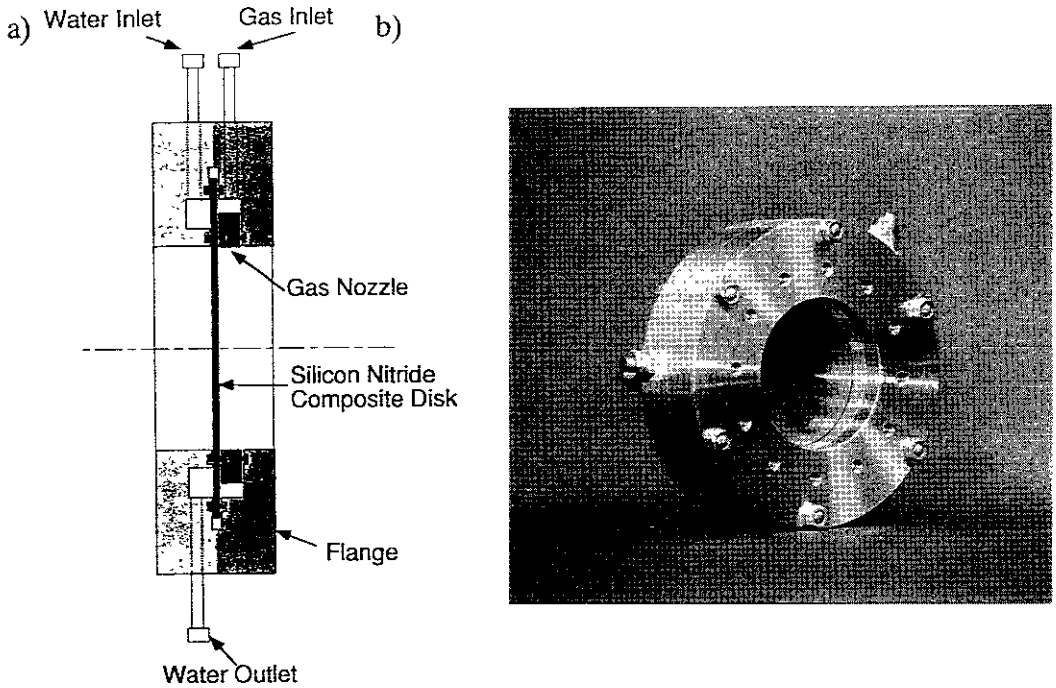

Fig. 1 a) Structure of the forced gas-cooled single-disk window of a silicon nitride composite.
b) Photograph of the window.

Using the low loss silicon nitride composite, we assembled a forced gas-cooled single-disk window with an edge-water cooling. Figure 1 (a) shows the structure of the gas-cooled single-disk window for high power testings. A circular disk of the silicon nitride composite with a diameter of 150mm and a thickness of about 2mm is held between two stainless steel flanges and sealed by O-rings. In this window structure, the whole surface of one side is forced gas-cooled by means of gas erupting nozzles perforated on the inner wall of the flange and the disk edge of another side is water-cooled. The typical diameter of the holes is 1mm and the number is 24. The nozzle section is exchangeable to check the effect of the size, the number of the holes and its configuration. A photograph of the window is shown in Fig. 1 (b). The effective diameter of the window is 88.9mm and can be connected to a corrugated waveguide with the same inner diameter. Working gases used for testings are dry nitrogen and dry air.

3. Experimental setup

For the high power transmission/absorption testings through the window, we used a high power test-stand which consists of an 84GHz high power CW gyrotron, several meters transmission lines, some quasi-optical components and a CW dummy load.

The power source is an 84GHz gyrotron which has an ability of 500kW 2sec., 400kW 10.5sec., 200kW 30sec. and 100kW 30min. operations[3]. Normal operation for the window testings is conducted at 100-200kW power level. The output from the gyrotron which has a flattened RF profile with a peaking factor of about 4.5 is coupled to an HE_{11} mode in a corrugated waveguide by two focusing mirrors and transmitted over about 3.4m through two miter bends.

Figure 2 illustrates the 84GHz high power window test-stand. The millimeter-wave power introduced into the corrugated waveguide is transmitted through the window under test, coupled into a dummy load by another set of two mirrors in a matching mirror box. Transmitted power through the window was measured by this dummy load. Temperature profiles and the peak temperature of the window were monitored by an IR camera through a port equipped on the matching mirror box. The readings of the IR temperature were directly calibrated by a Pt thermometer in advance. The cooling gas was supplied from a gas cylinder and its flow rate was measured by a float type area flow meter.

With gas-cooling the total absorbed power in the window disk is divided into two portions in the steady state. One is the power removed by heat conduction, which is estimated by a temperature rise of cooling water of the disk. Another is the power removed by gas cooling. The total absorbed power corresponds to the removed one without gas-cooling.

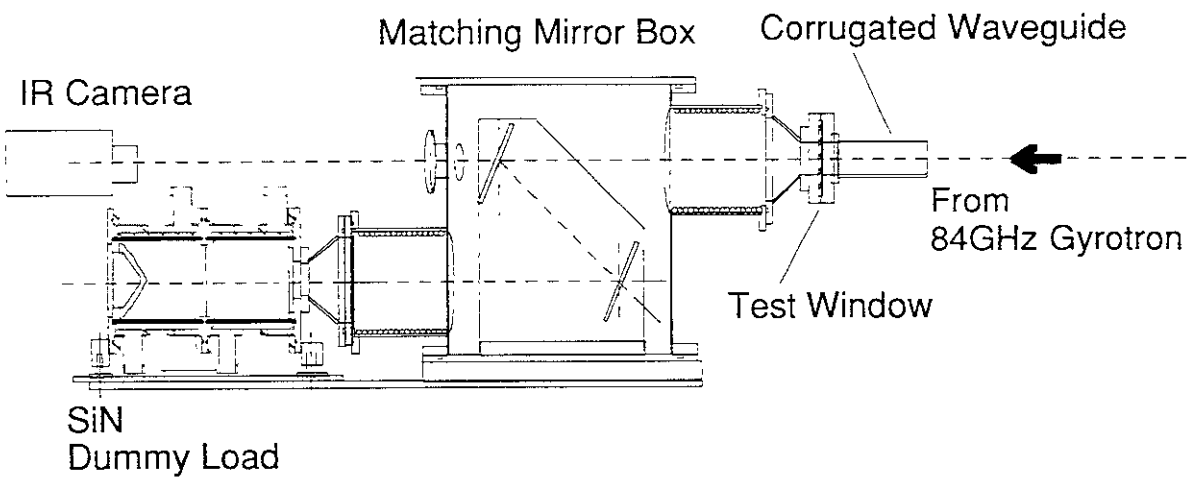

Figure 2 Schematic view of the 84GHz high power window transmission test-stand.

4. Experimental Results

At first we used a 2.53mm thickness disk which corresponded to twice of the wavelength in the disk. The gyrotron was operated at a high repetition rate of 10Hz and 150kW power level. Average input power to the window was changed by increasing the pulse width up to 30msec, corresponding to 30% duty.

Figure 3 shows the dependence of peak temperature rise on the average input power with and without gas-cooling of dry nitrogen. Without gas-cooling, the saturated peak temperature of the window disk increased rapidly with the increase of the average input power. Above 50kW, a phenomenon of thermal runaway seems to occur. By gas-cooling of only 104 liter/min., however, the saturated peak temperature was reduced drastically.

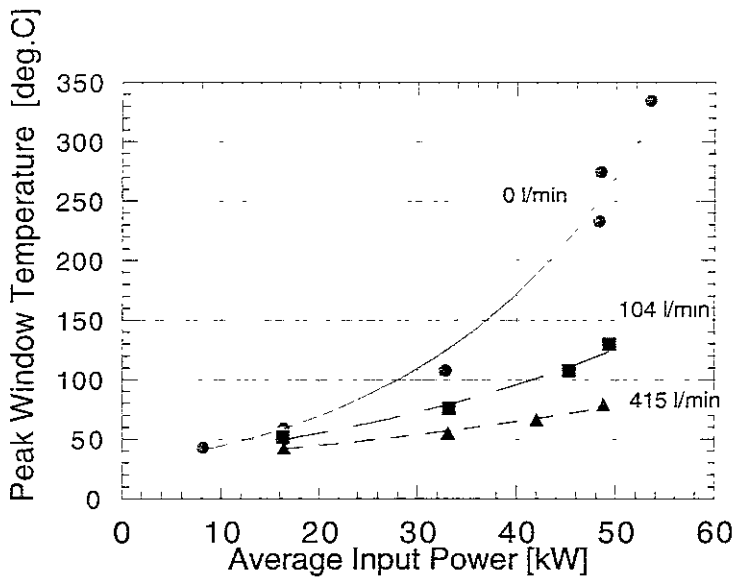

Figure 3 Dependence of peak window temperature on average input power for several gas nitrogen flow rates.

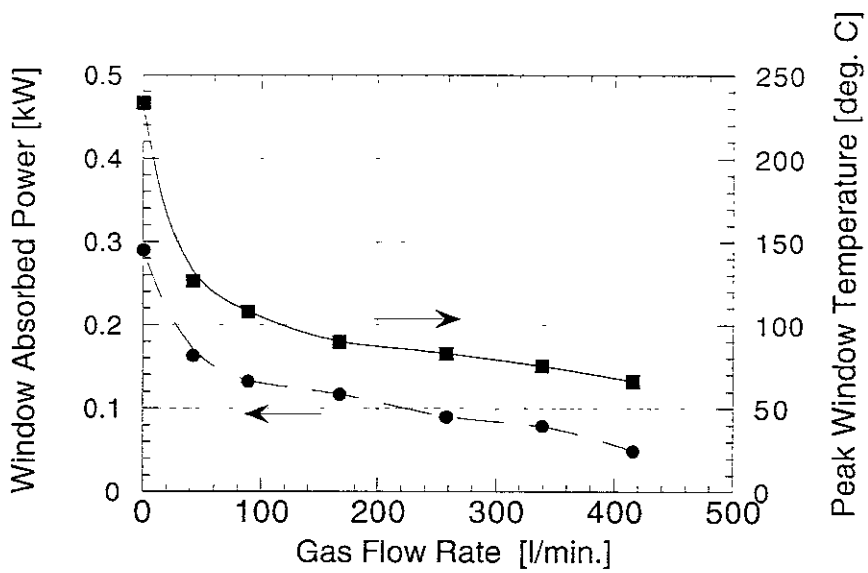

Figure 4 Dependence of peak window temperature and absorbed power in the window on gas flow rate. In this case, the input power is about 150kW and duty factor is 30%.

The power removed by heat conduction in the disk and maximum temperature on the disk are plotted as a function of the gas flow rate for 30% duty and around 150kW peak power injection in Fig. 4. Both have the same dependences on the gas flow rate. The effect of gas-cooling is great in the range of 100 liter/min. flow.

In order to demonstrate a possibility of a high power CW window, we performed 30 seconds injection with 130kW power. In this case we used the disk of 1.9mm thickness which corresponded to one and half of the wavelength. This disk has a lower loss tangent value than the disk of 2.53mm thickness. Figure 5 shows the time evolution of the peak temperature on the disk with and without gas-cooling. Without gas-cooling it continued to increase during the pulse, because of the inferiority of the thermal conductivity. At the end of the 30sec. pulse the maximum temperature reached as high

as 323 °C. On the other hand, with forced gas-surface-cooling of 465 liter/min., the peak temperature completely saturated during the pulse. The saturated temperature is 123.6 °C. This fact means that this type of the window can withstand a 130kW CW power transmission of HE_{11} mode through the waveguide with 88.9mm in diameter.

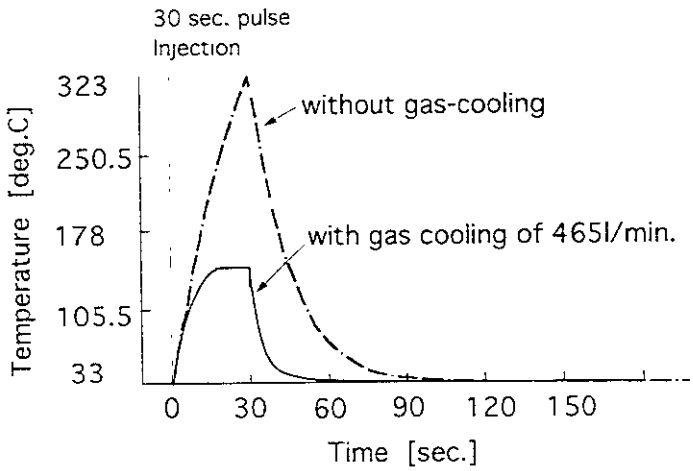

Figure 5 Time evolution of the peak temperature on the disk during 130kW, 30sec. injection without gas-cooling and with gas-cooling of 465l/min.

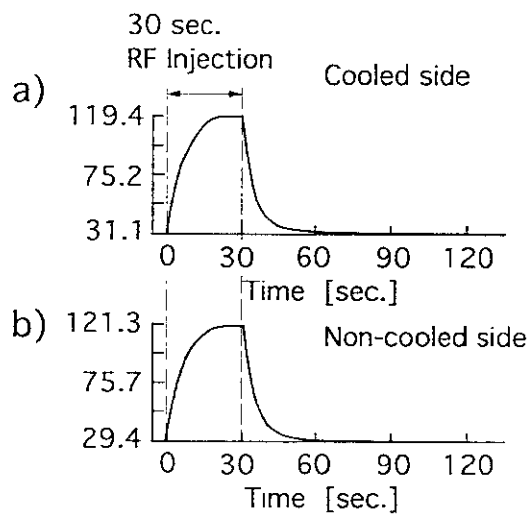

Figure 6 Comparison between temperature time evolution on the front (gas-cooled) side (a) and the back (non-cooled) side (b) of the silicon nitride disk for a 120kW 30sec. pulse injection.

A big temperature difference and a steep temperature gradient between the cooled and non-cooled sides of the disk sometimes leads to a fracture of the window material. We measured temperature profiles on each side as shown in Fig. 6. A 120kW 30sec. power was injected into the gas-cooled Si_3N_4 disk. Time evolution of the temperatures on both sides was measured by the IR camera. With gas-cooling both temperatures reached and saturated at a temperature of about 120 °C, and could not be noticed much differences. The result from thermal analysis is consistent with these experimental results.

5. Discussion

5.1 Estimation of the heat transfer coefficient

The local heat transfer coefficient of the forced gas-cooling can be estimated by means of evaluating the decay time of the peak temperature on the disk after turning off of a millimeter-wave injection. The temporal behavior of the temperature T at a given point is simply described as

$$\begin{aligned}\frac{\partial T}{\partial t} &= \frac{h}{\gamma C d}\left(T_f - T\right) + \frac{\lambda}{\gamma C}\nabla^2 T \\ &\equiv \frac{1}{\tau_0}\left(T_f - T\right)\end{aligned}, \qquad (1)$$

where Tf is an asymptotic temperature and γ , C, λ represent a mass density, specific heat and thermal conductivity, respectively. d corresponds to disk thickness and h is the heat transfer coefficient. The measured decay time constant τ_0 is a combination of two ways of the heat transport as shown in the second equation of Eq. (1)

Since the evolution of the disk temperature caused by the heat transfer can not be distinguished from that by the heat conduction experimentally, we evaluated the decay time constants τ_0 for some given heat transfer coefficients by the finite element thermal analysis code (ANSYS) on the same disk configuration and for the equivalent boundary conditions. Figure 7 (a) illustrates the configuration and boundary conditions of the calculation. First an initial temperature distribution was established by 30 seconds RF injection. After turned off the RF power, the temperature decay was pursued with a given heat transfer coefficient h. The relation between the 1/e decay time and the assumed heat transfer coefficient h is plotted in Fig. 7 (b). Using this correspondence, we can estimate the heat transfer coefficient h from the values of τ_0 obtained experimentally. In Fig. 8, the heat transfer coefficient estimated by the above described manner are plotted as a function of the gas flow rate. The coefficient h increases gradually with the gas flow rate and are fitted well with a 4/5 power curve of the gas flow rate normalized adequately as shown by a dotted curve in Fig. 8. The reason is that the heat transfer coefficient is roughly proportional to a 4/5 power of the Reynolds number which is related with the flow speed i.e. flow rate as will be shown in the next sub-section. The maximum value of the heat transfer coefficient is achieved to 0.1 W/cm^{2}K which reaches as high as one thirds of the value of an FC-75 surface-cooling with a flow rate of 42 liter/min. The heat transfer coefficient on zero flow rate corresponds to the heat transfer by a natural convection.

a)

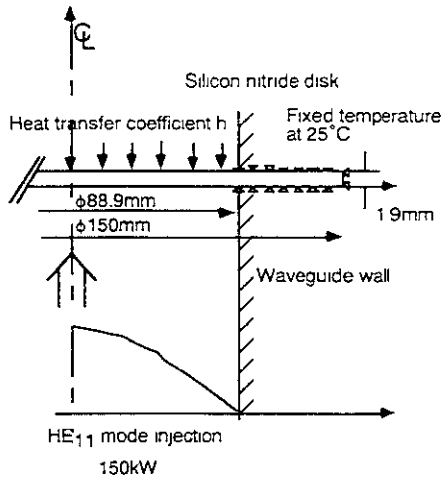

b)

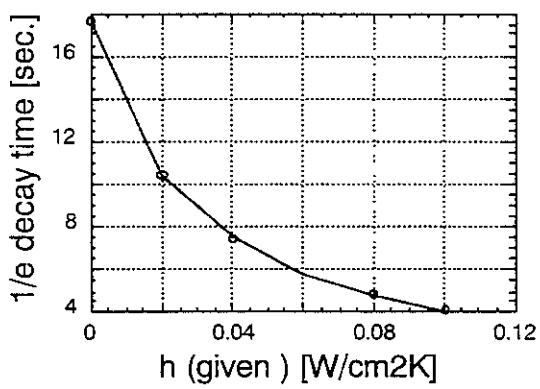

Figure 7 Configuration and boundary condition for the thermal analysis on the basis of finite element method a). For a given heat transfer coefficient 1/e decay time constant is plotted in b).

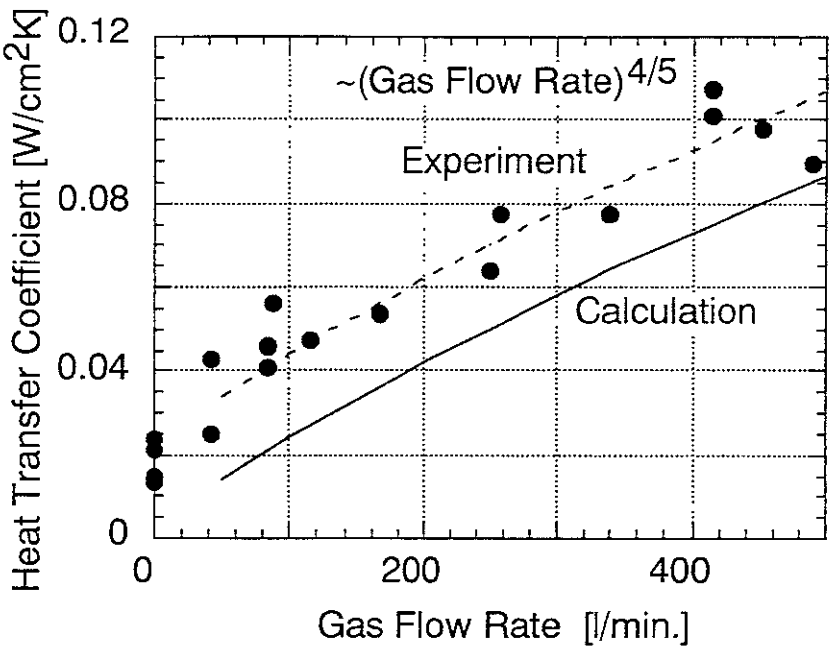

Figure 8 Estimated heat transfer coefficient as a function of the gas flow rate together with calculation result by Eq. (2).

5.2 Comparison of heat transfer coefficient from experimental data with the estimations from the empirical formula

For the gas flow rate of over 100 liter/min. the random flow seems to be established from its Reynolds number. A heat transfer coefficient for the random flow is described by following Johnson-Rubesin formula[12].

$$N_{ux} = 0.0296 P_r^{2/3} R_e^{4/5}, \tag{2}$$

where N_{UX}, P_r, R_{ex} are Nusselt, Plandtl and Reynolds numbers and given by

$$N_{ux} = \frac{hx}{\lambda}, \quad P_r = \frac{\eta c_p}{\lambda}, \quad R_{ex} = \frac{U_\infty x}{\nu}, \tag{3}$$

where h is a heat transfer coefficient and λ, η, ν are a thermal conductivity, viscosity and kinematic viscosity of a working gas, respectively. C_p denotes a specific heat at constant pressure. U_∞ represents a flow speed and x is a characteristic length of the configuration. Equation 2 is valid for the parameter range of $0.5<P_r<5$.

Assuming a gas nitrogen flow from one nozzle of 1mm in diameter, choosing the radius of the window as the characteristic length x, and taking the material parameters into account, we can obtain the heat transfer coefficient h from eqs.(2),(3). The calculated curve is also plotted in Fig. 8, which is consistent with the experimental results except a gap at zero gas flow rate.

Table 2 Dependence of the heat transfer coefficient on gas species with their physical properties at 0.1MPa and 300K. In the calculation gas flow speed is assumed to be 400m/sec. and characteristic length x is 4cm.

Gas species	Density ρ kg/m³	Thermal conductivity λ W/mK ×10⁻³	Specific heat Cp J/kgK ×10³	Viscosity η Pa s ×10⁻⁶	Kinematic viscosity ν m²/s ×10⁻⁶	Reynolds number Re	Plandtl number Pr	Nusselt number Nu	Heat transfer coeff. h W/m²K
H2	0.08	181.00	14.31	8.96	110.62	1.446E+05	0.7084	316	1430
He	0.16	153.00	5.19	19.90	124.38	1.286E+05	0.6750	279	1066
N2	1.13	26.00	1.04	17.90	15.90	1.006E+06	0.7160	1502	977
Air	1.16	26.14	1.01	18.62	16.04	9.976E+05	0.7173	1494	976
O2	1.28	26.30	0.92	20.70	16.12	9.925E+05	0.7241	1497	984
CO2	1.77	16.60	0.85	14.90	8.42	1.901E+06	0.7630	2607	1082

5.3 Dependence of the heat transfer coefficient on gas species

On the basis of the equation (2), the dependence of the heat transfer coefficient on gas species can be estimated. Table 2 presents the calculated heat transfer coefficient for several kinds of gases with their physical properties. Light molecules such as hydrogen and helium are more efficient than the others only on the aspect of the cooling efficiency.

As a gas coolant, suffocative, explosive and poisonous gases should be avoided to use in the gyrotron working space or a plasma experimental building. Otherwise, a closed recycling system of

the gases is required. A cooling and circulating system of much gas is, however, too expensive. Therefore, dry air is more attractive than nitrogen gas from a practical point of view.

We performed the same tests in which dry air was used as a coolant gas instead of nitrogen gas. No arcing occurred during 140kW, 30sec. power transmission. Peak temperature reached about 135 °C with a flow rate of 407 liter/min., while it was 154 °C with 409 liter/min. of nitrogen gas.

5.4 Brewster window

A Brewster window is advantageous for a reduction of mode competitions and tunable gyrotrons, because the incident angle at which the wave reflection completely disappears for a linearly polarized wave in the incident plane does not depend on the frequency, but only on the permittivity. From a viewpoint of high power windows, the Brewster window has a lot of merits. In addition to its frequency independence, it has an effectively large area and the power density of an injected RF beam can be reduced by several times. Being different from normally-injected resonant windows, the thickness of the Brewster window can be selected freely from the RF wavelength and determined from the aspect of mechanical designs. Most important point is re-adjustability by changing the inclination of the disk, because permittivities of sintering materials have a little difference between samples even at the same temperature, furthermore they have various temperature dependences. If a disk is heated up during a high power RF injection, the reflection from the window can be minimized by changing the disk inclination.

Its elliptical shape also has less internal stresses and smaller deformation than a circular shape with the same surface area. For instance, an elliptical disk with the elliptivity of 3 has about 60% maximum tensile stress and 30% deformation of a circular one with the same area and thickness.

For the silicon nitride composite with a permittivity of 7.92, the Brewster angle θ_B is 70.44°. When an elliptical disk is installed in a circular waveguide, the disk has an elliptivity of approximately three. Let's estimate the size of a 1MW CW window with this material and with the forced gas-cooling. Since a 130kW CW transmission is possible from the experimental results, 7.7 times of the disk area is required for 1MW, if the peaking factor of the incident wave are kept constant (about 3.7 for HE_{11} mode). This means that the size of 140 × 420 mm^2 will be necessary. The thickness of the disk will be about 3.5 mm, if the maximum tensile stress is suppressed below 100MPa, when the maximum deformation is expected to be 0.3mm.

6. Summary

The sintered silicon nitride composite has some superior characteristics such as low loss tangent and high mechanical toughness to sapphire. We use this composite material for high power millimeter-wave windows. Since a normal edge-cooled single-disk window is not sufficient to a several hundreds kilowatts or one megawatt CW transmission, we constructed a forced gas-cooled single-disk window with an edge-water-cooling. In this window structure, the surface of one side is forced gas-cooled from the gas erupting nozzles perforated on the inner wall of the window flange

and the disk edge on another side is water-cooled. High power transmission and absorption tests were performed by an 84GHz CW gyrotron. Following results are obtained.
(1) The gas-cooling dramatically suppressed the peak temperature of the window disk even with 100 liter/min gas flow rate. (2) A 130kW CW power of HE_{11} mode could be transmitted through the silicon nitride window with a effective diameter of 88.9mm. The peak window temperature was completely saturated on 123.6 °C, while without gas-cooling it continuously increased to 323 °C at the end of the RF pulse. (3) The estimated value of the heat transfer coefficient for the gas-cooling achieved to 0.1 W/cm^2K, which is comparable to as high as one thirds of the value of FC-75 surface-cooling with a 42 liter/min. flow. This estimation is consistent with the calculated results based on the empirical formula. (4) From a practical point of view, dry air could be used as a coolant in place of nitrogen gas. (5) We discussed a possibility of 1MW CW Brewster windows with gas-cooling and obtained the prospects of the windows with realistic size and thickness.

Finally we actually installed the silicon nitride composite disk to a 168GHz high power gyrotron for the first time in the world. Over 500kW power is extracted through the window during short pulse tests. Beforehand the analysis of the ingredient of outgases from the material at high temperature, metalizing and brazing tests with a copper and heat cycle tests were performed. Forced gas-cooling structure is now on preparation.

Acknowledgments

The authors would like to thank Mrs. K. Tajima and M. Sawai of Kyocera Corp. for fabricating the silicon nitride samples and for their valuable discussion, and Drs. Y. Okazaki and T. Okamoto of Toshiba Corp. for collaboration of a gyrotron window development and also express appreciation to Professors A. Iiyoshi and M. Fujiwara of NIFS for their continuous encouragement.

References

(1) T. Shimozuma, M. Sato, Y. Takita, S. Kubo, H. Idei, K. Ohkubo, T. Watari, S. Yasutomi, Y. Suzuki, F. Saito, S. Sasaki, Y. Saito and T. Okamoto, "Development *of an ECRH System for Large Helical Device"*, 19th Symposium on Fusion Technology, Sept. 16-20, 1996, Portugal, PB-8.

(2) K. Felch, M. Blank, P. Borchard, T. S. Chu, J. Feinstein, H. R. Jory, J. A. Lorbeck, C. M. Loring, Y. M. Mizuhara, J. M. Neilson,R. Schumacher and R. J. Temkin, *"Long-Pulse and CW Tests of a 110GHz Gyrotron with an Internal, Quasi-Optical Converter"*, IEEE Transaction on Plasma Science, 24 (1996) 558-569.

(3) M. Sato, T. Shimozuma, Y. Takita, S. Kubo, H. Idei, K. Ohkubo, T. Kuroda, T. Watari, M. Loring, Jr, S. Chu, K. Felch and H. Huey, "Development *of a High Power, 84GHz CW Gyrotron"*, Conference Digest of the 20th International Conference on Infrared and Millimeter Waves, Orlando, Florida, December 11-14, 1995 T4.3, pp195-196

(4) K. Felch, P. Borchard, P. Cahalan, T. S. Chu, H. Jory, C. M. Loring Jr. and C. P. Moeller, *"Status of 1MW, CW, Gyrotron Development at CPI"*, Conference Digest of the 21th International Conference on Infrared and Millimeter Waves, Berlin, Germany, July 14-19, 1996, AM16.

(5) C. P. Moeller, J. L. Doane and M. DiMartino, *"A Vacuum Window for a 1MW CW 110GHz Gyrotron"*, Conference Digest of the 19th International Conference on Infrared and Millimeter Waves, Sendai, October 17-20, 1994 W1.2, pp279-280.

(6) V. E. Mjasnikov, M. V. Agapova, V. V. Alikaev, A. S. Borshchegovsky, G. G. Denisov, V. A. Flyagin, A. Sh. Fix, V. I. Ilyin, V. N. Ilyin, A. P. Keyer, V. A. Khmara, D. V. Khmara, A. N. Kostyna, V. O Nichiporenko, L. G. Popov and V. E. Zapevalov, *"Megawatt power long-pulse 140GHz Gyrotron"*, Conference Digest of the 21th International Conference on Infrared and Millimeter Waves, Berlin, Germany, July 14-19, 1996, ATh1.

(7) A. Kasugai, K. Yokokura, K. Sakamoto, M. Tsuneoka, T. Yamamoto and T. Imai, *"High Power Tests of the Cryogenic Window for Millimeter Wave"*, Conference Digest of the 19th International Conference on Infrared and Millimeter Waves, Sendai, October 17-20, 1994 W2.3, pp295-296.

(8) S. Alberti, O. Braz, P. Garin, E. Giguet, M. pain, P. H. Thouvenin, M. Thumm, C. Tran and M. Q. Tran, *"Long Pulse Operation of a 0.5MW - 118GHz Gyrotron with Cryogenic Window"*, Conference Digest of the 21th International Conference on Infrared and Millimeter Waves, Berlin, Germany, July 14-19, 1996, AF1.

(9) V. V. Parshin, R. Heidinger, B. A. Andreev, A. V. Gusev and V. B. Shmagin, *"Silicon as an Advanced Window Material for High Power Gyrotrons"*, International Journal of Infrared and Millimeter Waves, 16 (1995) pp863-877.

(10) R. Heidinger, *"Dielectric Property Measurements on CVD Diamond Grades for Advanced Gyrotron Windows"*, Conference Digest of the 19th International Conference on Infrared and Millimeter Waves, Sendai, October 17-20, 1994 W1.1, pp277-278.

(11) T. Shimozuma, M. Sato, Y. Takita, S. Kubo, H. Idei, K. Ohkubo, T. Watari, S. Morimoto and K. Tajima, *"Development of Elongated Vacuum Windows for High Power CW Millimeter Waves"*, Conference Digest of the 20th International Conference on Infrared and Millimeter Waves, Orlando, Florida, December 11-14, 1995 T8.3, pp273-274.

(12) H. Martin, *Advances in Heat Transfer*, 13 (1977)1.

Recent Issues of NIFS Series

NIFS-468 A. Sagara, Y. Hasegawa, K. Tsuzuki, N. Inoue, H. Suzuki, T. Morisaki, N. Noda, O. Motojima, S. Okamura, K. Matsuoka, R. Akiyama, K. Ida, H. Idei, K. Iwasaki, S. Kubo, T. Minami, S. Morita, K. Narihara, T. Ozaki, K. Sato, C. Takahashi, K. Tanaka, K. Toi and I. Yamada,
Real Time Boronization Experiments in CHS and Scaling for LHD; Dec. 1996

NIFS-469 V.L. Vdovin, T.Watari and A. Fukuyama,
3D Maxwell-Vlasov Boundary Value Problem Solution in Stellarator Geometry in Ion Cyclotron Frequency Range (final report); Dec. 1996

NIFS-470 N. Nakajima, M. Yokoyama, M. Okamoto and J. Nührenberg,
Optimization of M=2 Stellarator; Dec. 1996

NIFS-471 A. Fujisawa, H. Iguchi, S. Lee and Y. Hamada,
Effects of Horizontal Injection Angle Displacements on Energy Measurements with Parallel Plate Energy Analyzer; Dec. 1996

NIFS-472 R. Kanno, N. Nakajima, H. Sugama, M. Okamoto and Y. Ogawa,
Effects of Finite-β and Radial Electric Fields on Neoclassical Transport in the Large Helical Device; Jan. 1997

NIFS-473 S. Murakami, N. Nakajima, U. Gasparino and M. Okamoto,
Simulation Study of Radial Electric Field in CHS and LHD; Jan. 1997

NIFS-474 K. Ohkubo, S. Kubo, H. Idei, M. Sato, T. Shimozuma and Y. Takita,
Coupling of Tilting Gaussian Beam with Hybrid Mode in the Corrugated Waveguide; Jan. 1997

NIFS-475 A. Fujisawa, H. Iguchi, S. Lee and Y. Hamada,
Consideration of Fluctuation in Secondary Beam Intensity of Heavy Ion Beam Prove Measurements; Jan. 1997

NIFS-476 Y. Takeiri, M. Osakabe, Y. Oka, K. Tsumori, O. Kaneko, T. Takanashi, E. Asano, T. Kawamoto, R. Akiyama and T. Kuroda,
Long-pulse Operation of a Cesium-Seeded High-Current Large Negative Ion Source; Jan. 1997

NIFS-477 H. Kuramoto, K. Toi, N. Haraki, K. Sato, J. Xu, A. Ejiri, K. Narihara, T. Seki, S. Ohdachi, K. Adati, R. Akiyama, Y. Hamada, S. Hirokura, K. Kawahata and M. Kojima,
Study of Toroidal Current Penetration during Current Ramp in JIPP T-IIU with Fast Response Zeeman Polarimeter; Jan., 1997

NIFS-478 H. Sugama and W. Horton,
Neoclassical Electron and Ion Transport in Toroidally Rotating Plasmas; Jan. 1997

NIFS-479 V.L. Vdovin and I.V. Kamenskij,
3D Electromagnetic Theory of ICRF Multi Port Multi Loop Antenna; Jan. 1997

NIFS-480 W.X. Wang, M. Okamoto, N. Nakajima, S Murakami and N. Ohyabu,
Cooling Effect of Secondary Electrons in the High Temperature Divertor Operation; Feb. 1997

NIFS-481 K. Itoh, S.-I. Itoh, H. Soltwisch and H.R. Koslowski,
Generation of Toroidal Current Sheet at Sawtooth Crash; Feb. 1997

NIFS-482 K. Ichiguchi,
Collisionality Dependence of Mercier Stability in LHD Equilibria with Bootstrap Currents; Feb. 1997

NIFS-483 S. Fujiwara and T. Sato,
Molecular Dynamics Simulations of Structural Formation of a Single Polymer Chain: Bond-orientational Order and Conformational Defects; Feb. 1997

NIFS-484 T. Ohkawa,
Reduction of Turbulence by Sheared Toroidal Flow on a Flux Surface; Feb. 1997

NIFS-485 K. Narihara, K. Toi, Y. Hamada, K. Yamauchi, K. Adachi, I. Yamada, K. N. Sato, K. Kawahata, A. Nishizawa, S. Ohdachi, K. Sato, T. Seki, T. Watari, J. Xu, A. Ejiri, S. Hirokura, K. Ida, Y. Kawasumi, M. Kojima, H. Sakakita, T. Ido, K. Kitachi, J. Koog and H. Kuramoto,
Observation of Dusts by Laser Scattering Method in theJIPPT-IIU Tokamak Mar. 1997

NIFS-486 S. Bazdenkov, T. Sato and The Complexity Simulation Group,
Topological Transformations in Isolated Straight Magnetic Flux Tube; Mar. 1997

NIFS-487 M. Okamoto,
Configuration Studies of LHD Plasmas; Mar. 1997

NIFS-488 A. Fujisawa, H. Iguchi, H. Sanuki, K. Itoh, S. Lee, Y. Hamada, S. Kubo, H. Idei, R. Akiyama, K. Tanaka, T. Minami, K. Ida, S. Nishimura, S. Morita, M. Kojima, S. Hidekuma, S.-I. Itoh, C. Takahashi, N. Inoue, H. Suzuki, S. Okamura and K. Matsuoka,
Dynamic Behavior of Potential in the Plasma Core of the CHS Heliotron/Torsatron; Apr. 1997

NIFS-489 T. Ohkawa,
Pfirsch - Schlüter Diffusion with Anisotropic and Nonuniform Superthermal Ion Pressure; Apr. 1997

NIFS-490 S. Ishiguro and The Complexity Simulation Group,
Formation of Wave-front Pattern Accompanied by Current-driven

Electrostatic Ion-cyclotron Instabilities; Apr. 1997

NIFS-491 A. Ejiri, K. Shinohara and K. Kawahata,
An Algorithm to Remove Fringe Jumps and its Application to Microwave Reflectometry; Apr. 1997

NIFS-492 K. Ichiguchi, N. Nakajima, M. Okamoto,
Bootstrap Current in the Large Helical Device with Unbalanced Helical Coil Currents; Apr. 1997

NIFS-493 S. Ishiguro, T. Sato, H. Takamaru and The Complexity Simulation Group,
V-shaped dc Potential Structure Caused by Current-driven Electrostatic Ion-cyclotron Instability; May 1997

NIFS-494 K. Nishimura, R. Horiuchi, T. Sato,
Tilt Stabilization by Energetic Ions Crossing Magnetic Separatrix in Field-Reversed Configuration; June 1997

NIFS-495 T. -H. Watanabe and T. Sato,
Magnetohydrodynamic Approach to the Feedback Instability; July 1997

NIFS-496 K. Itoh, T. Ohkawa, S. -I.Itoh, M. Yagi and A. Fukuyama
Suppression of Plasma Turbulence by Asymmetric Superthermal Ions; July 1997

NIFS-497 T. Takahashi, Y. Tomita, H. Momota and Nikita V. Shabrov,
Collisionless Pitch Angle Scattering of Plasma Ions at the Edge Region of an FRC; July 1997

NIFS-498 M. Tanaka, A.Yu Grosberg, V.S. Pande and T. Tanaka,
Molecular Dynamics and Structure Organization in Strongly-Coupled Chain of Charged Particles; July 1997

NIFS-499 S. Goto and S. Kida,
Direct-interaction Approximation and Reynolds-number Reversed Expansion for a Dynamical System; July 1997

NIFS-500 K. Tsuzuki, N. Inoue, A. Sagara, N. Noda, O. Motojima, T. Mochizuki, T. Hino and T. Yamashina,
Dynamic Behavior of Hydrogen Atoms with a Boronized Wall; July 1997

NIFS-501 I. Viniar and S. Sudo,
Multibarrel Repetitive Injector with a Porous Pellet Formation Unit; July 1997

NIFS-502 V. Vdovin, T. Watari and A. Fukuyama,
An Option of ICRF Ion Heating Scenario in Large Helical Device; July 1997

NIFS-503 E. Segre and S. Kida,

Late States of Incompressible 2D Decaying Vorticity Fields; Aug. 1997

NIFS-504 S. Fujiwara and T. Sato,
Molecular Dynamics Simulation of Structural Formation of Short Polymer Chains; Aug. 1997

NIFS-505 S. Bazdenkov and T. Sato
Low-Dimensional Model of Resistive Interchange Convection in Magnetized Plasmas; Sep. 1997

NIFS-506 H. Kitauchi and S. Kida,
Intensification of Magnetic Field by Concentrate-and-Stretch of Magnetic Flux Lines; Sep. 1997

NIFS-507 R.L. Dewar,
Reduced form of MHD Lagrangian for Ballooning Modes; Sep. 1997

NIFS-508 Y.-N. Nejoh,
Dynamics of the Dust Charging on Electrostatic Waves in a Dusty Plasma with Trapped Electrons; Sep.1997

NIFS-509 E. Matsunaga, T.Yabe and M. Tajima,
Baroclinic Vortex Generation by a Comet Shoemaker-Levy 9 Impact; Sep. 1997

NIFS-510 C.C. Hegna and N. Nakajima,
On the Stability of Mercier and Ballooning Modes in Stellarator Configurations; Oct. 1997

NIFS-511 K. Orito and T. Hatori,
Rotation and Oscillation of Nonlinear Dipole Vortex in the Drift-Unstable Plasma; Oct. 1997

NIFS-512 J. Uramoto,
Clear Detection of Negative Pionlike Particles from H_2 Gas Discharge in Magnetic Field; Oct. 1997

NIFS-513 T. Shimozuma, M. Sato, Y. Takita, S. Ito, S. Kubo, H. Idei, K. Ohkubo, T. Watari, T.S. Chu, K. Felch, P. Cahalan and C.M. Loring, Jr,
The First Preliminary Experiments on an 84 GHz Gyrotron with a Single-Stage Depressed Collector; Oct. 1997

NIFS-514 T. Shimozuma, S. Morimoto, M. Sato, Y. Takita, S. Ito, S. Kubo, H. Idei, K. Ohkubo and T. Watari,
A Forced Gas-Cooled Single-Disk Window Using Silicon Nitride Composite for High Power CW Millimeter Waves; Oct. 1997